Modified Bloch equations and spectral hole burning in solids

2001 J. Phys.: Condens. Matter 13 5231

(http://iopscience.iop.org/0953-8984/13/22/316)

INSTITUTE OF PHYSICS PUBLISHING JOURNAL OF PHYSICS: CONDENSED MATTER

J. Phys.: Condens. Matter **13** (2001) 5231–5240 www.iop.org/Journals/cm PII: S0953-8984(01)22503-X

Modified Bloch equations and spectral hole burning in solids

N Ya Asadullina, T Ya Asadullin[1] and Ya Ya Asadullin

Kazan State Technical University, Department of General Physics, Karl Marx Street 10, Kazan 420111, Russia

E-mail: atimur@physics.kstu-kai.ru

Received 5 March 2001, in final form 19 April 2001

Abstract

On the grounds of Bloch equations modified by taking into account the power dependence of the dispersion and damping parameters, we give general expressions for hole shapes burnt in the absorption and polarization spectra of the two-level systems. The general expressions are used for detailed numerical calculations of the hole shapes and hole widths in a concrete paramagnetic system (quartz with $[AlO_4]^0$ centres). This system earlier was studied experimentally and theoretically through the transient nutation and free induction decay methods. The results on the hole width in our modified-Bloch-equations model are in good qualitative agreement with the FID data.

1. Introduction

The absorption lines of EPR transitions ω_0 in solids are inhomogeneously broadened. Hence, a monochromatic microwave field (pump field, saturation field) $H(\omega_s, t)$ resonantly excites only a small part of the spins within the inhomogeneously broadened spectral contour. As a result, we have a variation in the population: in the vicinity of $\omega_0 = \omega_s$ in the spectral distribution of the lower level one has a decrease of the concentration $n_1(\omega_0)$; i.e. a spectral hole is developed with the width approximately equal to the width of the saturated homogeneous absorption line. An example of such a spectral hole burnt under steady-state excitation by an mw field with Rabi frequency $\chi/2\pi = \gamma H/2\pi = 5$ kHz is shown in figure 1. Other conditions at which the figure is obtained will be described below. Accordingly, in the spectral distribution of the upper level one has an increase of the concentration $n_2(\omega_0)$: there appears a reverse hole. The small height of the holes in the figure (see the inset) is caused by the smallness of the polarization ($n_2 \approx n_1$). On the other hand, the spectral polarization itself, $p(\omega_0) \sim n_1(\omega_0) - n_2(\omega_0)$, which usually is of basic importance, has a sharp and deep minimum.

The information obtainable from the hole-burning studies is of the same kind as from the transient nutations (TN) [1], free induction decay (FID) [2] and spin echoes [3]. In particular, the half width at half maximum (or minimum) (HWHM) of the hole is approximately of the

[1] Corresponding author.

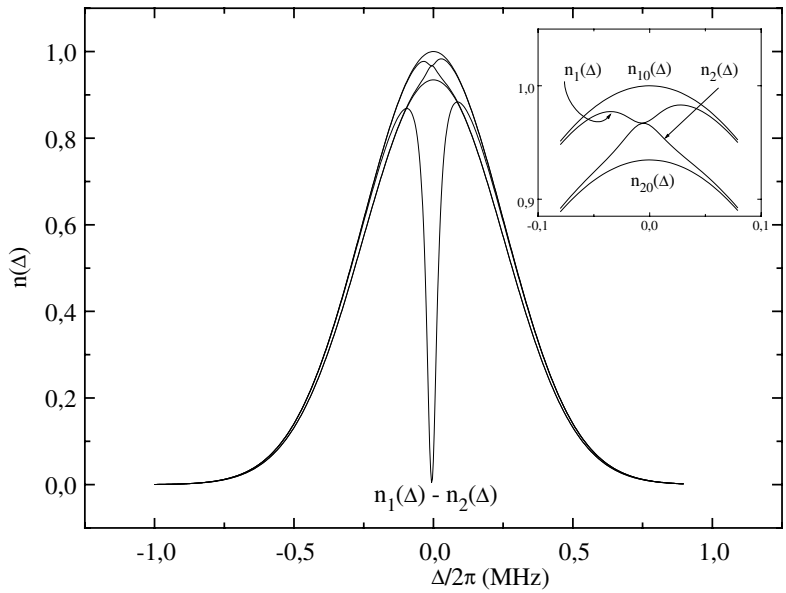

Figure 1. Hole burning in spectral distribution of spins at the ground level ($n_1(\Delta)$), reverse hole burning at the excited level ($n_2(\Delta)$), and in the spectral distribution of the polarization $\propto n_1(\Delta) - n_2(\Delta)$; $\chi/2\pi = 5$ kHz. The top part of the figure is shown in the inset on a larger scale.

same order as the FID rate in the same system. Hence, hole burning and the transient effects complement each other.

Theoretical description of TN, FID and spin echoes is usually based on the phenomenological Bloch equations. In the reference frame rotating with frequency ω_s, these equations are

$$\dot{u} + \Delta v + \frac{u}{T_{2u}} = 0 \qquad \dot{v} - \Delta u - \chi w + \frac{v}{T_{2v}} = 0 \qquad \dot{w} + \chi v + \frac{(w - w_0)}{T_1} = 0. \tag{1}$$

Ordinary Bloch equations (OBEs) (1) include two *power-independent* phenomenological relaxation parameters, T_1 and $T_{2u} = T_{2v} = T_2 = \Gamma_2^{-1}$, *power-independent* tuning parameter $\Delta = \omega_0 - \omega_s$, and the induced Rabi frequency $\chi = \gamma H$, where γ is the gyromagnetic ratio. For a two-level quantum system OBEs follow from the density-matrix equations of motion. In particular, we have

$$u = \rho_{12} + \rho_{21} \qquad v = \mathrm{i}(\rho_{21} - \rho_{12}) \qquad w = \rho_{22} - \rho_{11} \tag{2}$$

where ρ_{ij} is the ij-matrix element of the density matrix.

Experiments [1–3] on transient EPR effects in solids and similar experiments in optics [4–9] have shown, however, that OBEs fail in describing these effects. In particular, contrary to the predictions of the OBE model it follows from [1–9] that observed decay rates of the nutation, FID and echo responses are essentially intensity dependent. Based on these results, a somewhat modified version of the Bloch equations (MBEs) has been proposed in a recent paper [10] and used successfully to explain experimental results on TN [1] and FID [2]. In this paper we give, on MBE grounds, a theoretical description of the hole burning in the absorption spectrum of a two-level system by steady-state excitation. As a specific example, we perform detailed numerical calculations for sample no 1 of Boscaino and La Bella [2]

in both MBE and OBE models. Results of the line-width calculations are compared with observed [2] and calculated [10] FID rate data.

2. Modified Bloch equations

Hole burning can be examined, for example, through a scan of the inhomogeneous absorption spectrum by a small probe field $H_p(\omega_p, t)$. The absorption coefficient $\alpha(\omega_p)$ is given by

$$\alpha(\omega_p) = \frac{4\pi\omega_p}{c}\mathrm{Im}\,\chi(\omega_p) \qquad \chi(\omega_p) = \frac{n_0\mu_{12}\rho_{21}(\omega_p)}{H_p(\omega_p)}$$

where $\rho_{21}(\omega_p)$ is the Fourier component of the nondiagonal matrix element of the density matrix at frequency ω_p. Hence, one has to obtain $v(\omega_p) = 2\mathrm{Im}\,\rho_{21}(\omega_p)$ as a solution of the corresponding Bloch equations.

Below we briefly summarize the main features of the MBE model [10]. In distinction to OBEs, here tuning parameter $\Delta = \Delta(\chi)$ is power dependent; also, instead of a single constant relaxation parameter T_2 for transverse components one has power-dependent parameters $T_{2u}(\chi)$ [11] and $T_{2v}(\chi)$ for u and v components respectively. For steady-state excitation, the explicit form of $\Delta(\chi)$, $T_{2u}(\chi)$ and $T_{2v}(\chi)$ is as follows:

$$\Delta(\chi) = \Delta_0 + \omega + \delta\omega(\chi)$$

$$\delta\omega(\chi) = a_\omega\delta M_z = a_\omega\int_{-\infty}^{\infty}[w_0 - w(\Delta)]\delta n_2(\Delta)\,\mathrm{d}\Delta \tag{3}$$

$$\delta n_2(\Delta) = \left(\frac{n_0}{2} - n_{20}\right)\frac{S(\Delta,\chi)}{1+S(\Delta,\chi)}g(\Delta) \qquad S(\Delta,\chi) = \frac{T_1\Gamma_{2v}\chi^2}{4\Delta^2+\Gamma_{2v}^2} \tag{4}$$

$$\Gamma_{2u} = \frac{\Gamma_0}{1+r^2\chi^2} + \frac{1}{2T_1} \tag{5}$$

$$\Gamma_{2v} = \Gamma_0\left[1 + \frac{1}{2T_1\Gamma_0}\right] + a_\Gamma\int[u^2(\Delta)+v^2(\Delta)]^{1/2}\delta n_2(\Delta)\,\mathrm{d}\Delta. \tag{6}$$

In equations (3) $\omega = \omega_0 - \omega_{00}$ measures the spectral distance of the generic spin (ω_0) from the central frequency of the inhomogeneously broadened line ω_{00}; $\Delta_0 = \omega_{00} - \omega_s$ and for centre excitation $\Delta_0 = 0$. Further, $\delta\omega(\chi)$ gives the intensity-dependent shift of the transition frequency due to change in the z-component of the local magnetic field with parameter a_ω proportional to demagnetizing coefficient N. It is assumed [1–3] that the inhomogeneously broadened resonance line has a Gaussian profile with a standard deviation σ:

$$g(\omega) = (2\pi)^{-1/2}\sigma^{-1}\exp(-\omega^2/2\sigma^2). \tag{7}$$

The change in spectral concentration of the upper level $\delta n_2(\Delta) = n_2(\Delta) - n_{20}(\Delta)$ is obtained as the steady-state solution of the standard rate equation

$$\dot{n}_2(\Delta,t) = -(w_{21}+W_{21})n_2(\Delta,t) + (w_{12}+W_{12})n_1(\Delta,t)$$

$$n_1(\Delta,t) + n_2(\Delta,t) = n(\Delta) = n_0 g(\Delta) \qquad n_1 + n_2 = n_0. \tag{8}$$

Here w_{21} is the transition probability per second for a spin from excited level 2 to ground level 1, w_{12} is the probability for the reverse process, $W_{21} = 2\pi\chi^2 g_L(\omega)$ and W_{12} are the probabilities for induced transitions $1 \leftrightarrow 2$ and $g_L(\omega)$ is the usual Lorentzian profile. In equation (4) $S(\Delta,\chi)$ is the spectral saturation parameter. In (5) r is the parameter associated with the correlation time of dipole–dipole interactions [11]. The first term on the right-hand side of equation (6) describes the contribution to the damping from the thermally excited spins and from the spin–lattice interaction; the last term is due to the coherently excited spins.

Parameters $\Delta(\chi)$ (3) and Γ_{2v} (6) depend on $u(t)$, $v(t)$ and $w(t)$, so the modified Bloch equations are inherently nonlinear. Since required parameters $\delta\omega(\chi)$, Γ_{2v}, $\delta n_2(\Delta, t)$ and variables $u(t)$, $v(t)$, $w(t)$ are interrelated, we construct $\delta n_2(\Delta)$, $\delta\omega$ and Γ_{2v} by the method of iteration. In the zeroth approximation ($k = 1$), for $u(t)$, $v(t)$ and $w(t)$ we use the well known steady-state solution [12]

$$u^{(0)} = \frac{\Delta\chi w_0 T_{2u} T_{2v}}{D} \qquad v^{(0)} = -\frac{\chi w_0 T_{2v}}{D} \qquad w^{(0)} = \frac{(1 + \Delta^2 T_{2u} T_{2v}) w_0}{D}$$
$$D = 1 + \Delta^2 T_{2u} T_{2v} + \chi^2 T_1 T_{2v} \tag{9}$$

where $T_{2u} = \Gamma_{2u}^{-1}$ is given by (5), $T_{2v} = T_2$ and $\Delta = \omega$.

Solution (9) is used in equations (3), (4), (6) to obtain improved expressions for $\delta n_2(\Delta)$, $\delta\omega$ and Γ_{2v}; the latter are, in turn, inserted into equations (9) and so on. Really, the expressions for $\delta\omega$ and Γ_{2v} get their final form after five cycles and do not vary further.

3. Hole burning

3.1. Theory

We start with the equation of motion for the density matrix

$$\mathrm{i}\hbar\dot{\rho} = [H', \rho] + \mathrm{i}\hbar \left(\frac{\partial\rho}{\partial t}\right)_{random}$$
$$\left(\frac{\partial\rho_{nn'}}{\partial t}\right)_{random} = -\Gamma'\rho_{nn'} \qquad \left(\frac{\partial\rho_{nn}}{\partial t}\right)_{random} = -\frac{1}{T_1}\rho_{nn}$$
$$H' = H_0' + H_{int}' \qquad H_{int}' = \mu_{21}(H\mathrm{e}^{-\mathrm{i}\omega_s t} + h_p\mathrm{e}^{-\mathrm{i}\omega_p t} + \mathrm{c.c.})$$

where H_0' is the unperturbed Hamiltonian of the two-level system with transition frequency $\omega_{21} = -\omega_{12} = \omega_0 = \omega_{00} + \omega + \delta\omega(\chi)$. Damping parameter Γ' can be expressed, using equations (1) and (2), in terms of Γ_{2u} and Γ_{2v} (see equations (10) below).

Following the work of Bloembergen and Shen [13], we seek the steady-state solution of this equation in the laboratory frame of coordinates. Since the interaction Hamiltonian $H_{int}' = \sum_j H_{int}'(\omega_j)$ is a set of the Fourier components, the density matrix can be expanded in the Fourier series as well: $\rho = \sum_j \rho(\omega_j)$. In the case of the steady-state excitation, the differentiation at the left-hand side of the equation of motion for a component $\rho(\omega_j) \sim \exp(-\mathrm{i}\omega_j t)$ is reduced to multiplication by $(-\mathrm{i}\omega_j)$. The coupled set of equations for the Fourier components of the matrix elements $\rho_{21}(\omega_p)$, $\rho_{12}(\omega_p - 2\omega_s)$ and $(\rho_{22} - \rho_{11})(\omega_p - \omega_s)$ is

$$(\omega_p - \omega_0\ddot{y} + \mathrm{i}\Gamma_+)\rho_{21}(\omega_p) + \mathrm{i}\Gamma_-\rho_{12}(\omega_p - 2\omega_s) - \chi_{21}(\rho_{22} - \rho_{11})(\omega_p - \omega_s)$$
$$= \chi_{p21}(\rho_{22} - \rho_{11})^{const}$$
$$-2\chi_{12}^*\rho_{21}(\omega_p) + 2\chi_{21}\rho_{12}(\omega_p - 2\omega_s) + \left(\omega_p - \omega_s\frac{\mathrm{i}}{T_1}\right)(\rho_{22} - \rho_{11})(\omega_p - \omega_s)$$
$$= -2\chi_{p21}\rho_{12}(-\omega_s)$$
$$\mathrm{i}\Gamma_-\rho_{21}(\omega_p) + (\omega_p - 2\omega_s + \omega_0 + \mathrm{i}\Gamma_+)\rho_{12}(\omega_p - 2\omega_s) + \chi_{12}^*(\rho_{22} - \rho_{11})(\omega_p - \omega_s) = 0$$
$$\chi_{21} = \hbar^{-1}\mu_{21}H \qquad \chi_{p21} = \hbar^{-1}\mu_{21}H_p. \tag{10}$$

In distinction to [13], here ω_0 is power dependent and by use of

$$\Gamma_\pm = \tfrac{1}{2}(\Gamma_{2u} \pm \Gamma_{2v})$$

the difference of the relaxation parameters for u- and v-components is taken into account.

Fourier components $(\rho_{22}-\rho_{11})^{const}$ and $\rho_{12}(-\omega_s)$ in (10) are evaluated from the equation of motion for the density matrix without considering the probe field and are given by

$$\rho_{12}(-\omega_s)=\frac{D_s}{D_{s0}} \qquad (\rho_{22}-\rho_{11})^{const}=\frac{D_c}{D_{s0}}$$
$$D_s=-\frac{\mathrm{i}}{T_1}[\mathrm{i}\chi_{21}\Gamma_- + \chi_{12}^*(\omega_s-\omega_0+\mathrm{i}\Gamma_+)](\rho_{22}^0-\rho_{11}^0)$$
$$D_c=-\frac{\mathrm{i}}{T_1}[(\omega_s-\omega_0)^2+\Gamma_+^2+\Gamma_-^2](\rho_{22}^0-\rho_{11}^0)$$
$$D_{s0}=-\frac{\mathrm{i}}{T_1}[(\omega_s-\omega_0)^2+\Gamma_+^2-\Gamma_-^2+4T_1\Gamma_+|\chi|^2+2T_1\Gamma_-(\chi_{21}^2+\chi_{12}^{*2})]. \qquad (11)$$

Here $(\rho_{22}^0-\rho_{11}^0)$ is the equilibrium (thermal) polarization of the spin system.

The solution of equations (10) for $\rho_{21}(\omega_p)$ is

$$\rho_{21}(\omega_p)=\frac{D_{sp}}{D_{s1}}$$
$$D_{sp}=\chi_{p21}\{[2|\chi|^2-(\omega_p-\omega_s+\mathrm{i}T_1^{-1})(\omega_p-2\omega_s+\omega_0+\mathrm{i}\Gamma_+)](\rho_{22}-\rho_{11})^{const}$$
$$+2\chi_{21}\rho_{12}(-\omega_s)(\omega_p-2\omega_s+\omega_0+\mathrm{i}\Gamma_+)+2\mathrm{i}\Gamma_-\chi_{12}^*\rho_{12}(-\omega_s)\}$$
$$D_{s1}=4|\chi|^2(\omega_p-\omega_s+\mathrm{i}\Gamma_+)+2\mathrm{i}\Gamma_-(\chi_{21}^2+\chi_{12}^{*2})-\Gamma_-^2(\omega_p-\omega_s+\mathrm{i}T_1^{-1})$$
$$-(\omega_p-\omega_0+\mathrm{i}\Gamma_+)(\omega_p-\omega_s+\mathrm{i}T_1^{-1})(\omega_p-2\omega_s+\omega_0+\mathrm{i}\Gamma_+). \qquad (12)$$

For the inhomogeneously broadened line, expressions (10)–(12) are related to a spin packet with the resonance frequency ω_0, so any packet has its own value of $\rho_{21}(\omega_p,\omega_0)=\rho_{21}(\omega_p,\omega)$. Therefore, the absorption coefficient is obtained by integration of $(\rho_{21}(\omega_p,\omega)+\rho_{21}(\omega_p,-\omega))/2$ over the inhomogeneous contour $g(\omega)$ (2).

With the pump field switched off, the spectral picture produced by the field survives for times of the order of T_1. For sufficiently large T_1 [14] this permits scanning the inhomogeneous contour by the probe field in the absence of $H(\omega_s,t)$. From the coupled equations for $\rho_{12}(-\omega_p)$ and $\rho_{21}(\omega_p)$ it is easy in this case to obtain

$$\mathrm{Im}\,\rho_{21}(\omega_2;\ H(\omega_s)=0)=\frac{\chi_p(\Gamma_++\Gamma_-)(\rho_{11}-\rho_{22})^{const}}{[(\omega_2-\omega_0)^2+\Gamma_+^2-\Gamma_-^2]} \qquad (13)$$

where, as before, $(\rho_{11}-\rho_{22})^{const}$ is given by formulae (11).

For comparison, it is pertinent to consider analogous expressions for $\rho_{21}(\omega_p)$ in the framework of the OBEs. They are obtained from (11)–(13) with substitutions $\omega_0=\omega_{00}+\omega$, $\Gamma_+=\Gamma_0$, $\Gamma_-=0$ there.

3.2. Numerical calculations and discussion

For numerical study of the hole properties through expressions (12) and (13), we need specific values of parameters that appear in these expressions. It is important here that both the hole-burning and FID effect are the consequences of one and the same resonance transition in the sample caused by the same steady-state excitation. Hence, in calculations below one can exploit the values of parameters known from FID studies. As an example, we apply the calculations to sample no 1 (quartz with $[AlO_4]^0$ centres) of Boscaino and La Bella [2].

Figures 2(*a*) and (*b*) depict the evolution of the calculated absorption coefficient $\alpha(\chi,\omega_p)$ for the probe field with increasing pump field $H(\omega_s,t)$ in the framework of the MBEs in the presence of $H(\omega_s,t)$ (*a*) and in its absence (*b*). In each case, the Rabi frequency of the pump field is varied in the range 0.1 kHz $\leqslant \chi/2\pi \leqslant$ 200 kHz from top to bottom. Coefficient

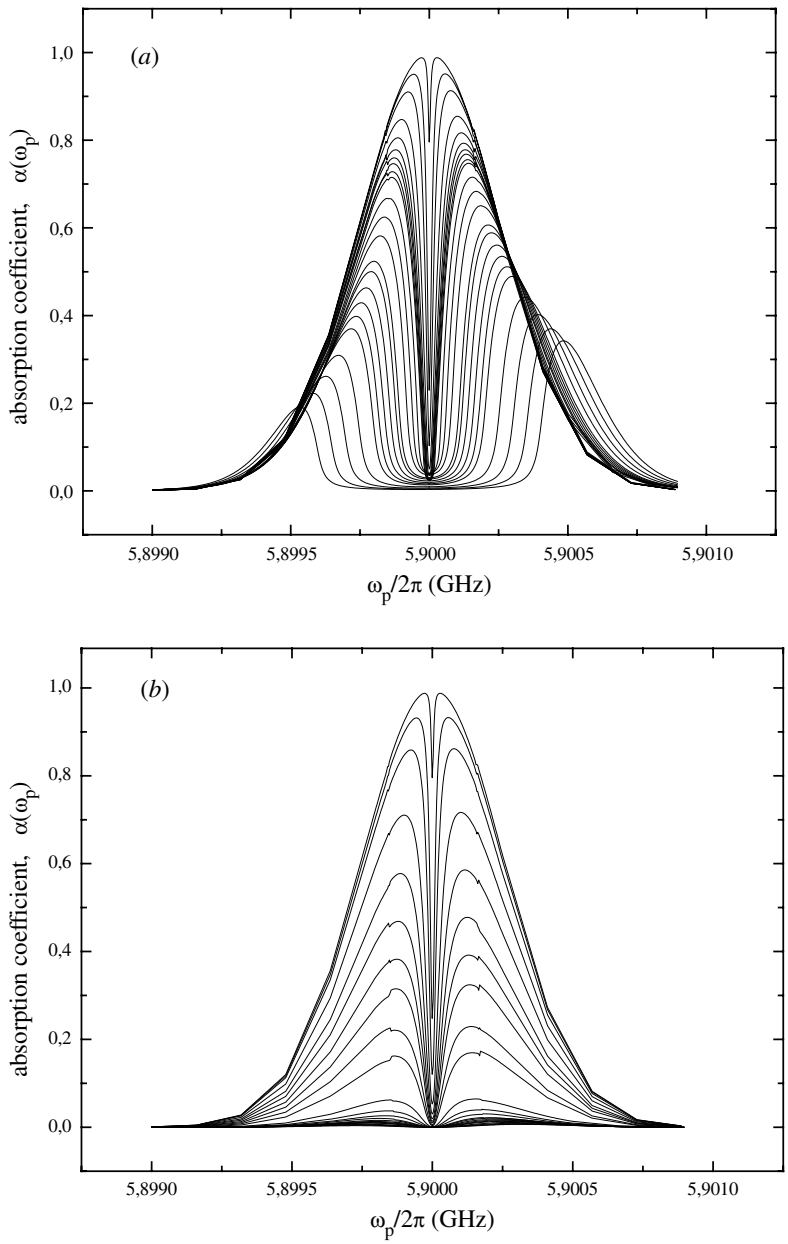

Figure 2. Evolution of the hole in absorption spectrum of a weak probe field in the modified Bloch model. From the top curve to the bottom one the pump-field Rabi frequency varies in the range 0.1 kHz $\leqslant \chi/2\pi \leqslant$ 200 kHz; (*a*) in the presence of the pump field, (*b*) when the pump field is switched off.

$\alpha(\chi, \omega_p)$ is normalized to unity for $\omega_p = \omega_{00} = \omega_s$ ($\omega_s/2\pi = 5.9$ GHz [2]) at vanishing values of χ. The values of the parameters used in these calculations are those obtained in [2] and [10] from the FID studies: $a_\omega = 3\times10^{-8}\,\mathrm{cm}^{-3}\,c^{-1}$, $a_\Gamma = 2.76\times10^{-8}\,\mathrm{cm}^{-3}\,c^{-1}$, $r^2 = 2\times10^{-9}\,c^2$, $T_1 = 5\times10^{-3}\,c$, $T_2 = \Gamma_0^{-1} = 7.5\times10^{-5}\,c$, $n_0 = 4\times10^{16}\,\mathrm{cm}^{-3}$ and $\sigma/2\pi = 0.25$ MHz.

In all calculations the Rabi frequency of the probe field $\chi_p/2\pi = 0.01$ kHz. With increasing pump field H the hole width in figure 2 monotonically increased and the hole height decreased. The existence of the power-dependent frequency shift and damping in our model introduces an asymmetry to the hole shape relative the central frequency as is clearly seen in figure 2(a) and less obviously in figure 2(b) (see curve b in figure 3 below). With increasing field intensity, the asymmetry increases as well. The curves in analogous figures of the OBE model (not shown here) are, in general, of symmetrical form (curves c and d in figure 3).

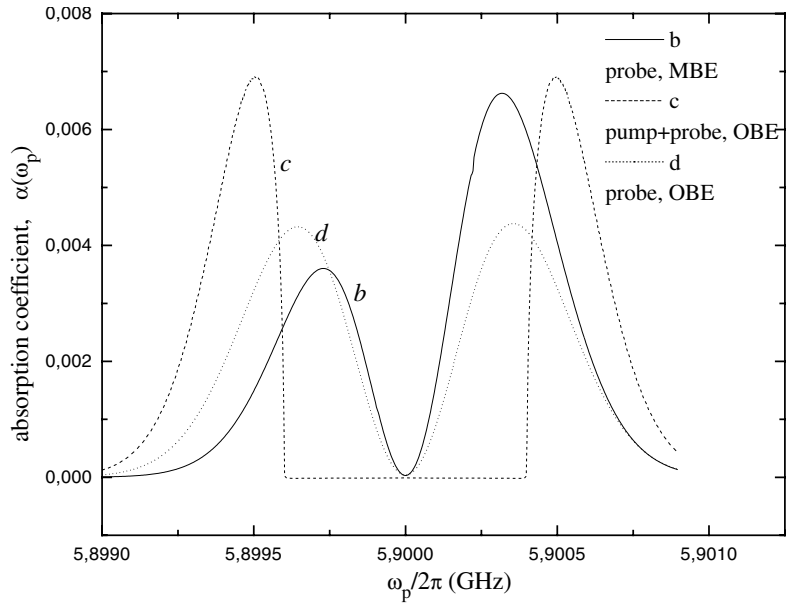

Figure 3. Hole in the absorption spectrum of a weak probe field for $\chi/2\pi = 200$ kHz in the MBE model (b) and in the OBE model (c and d). c is in the presence of the pump field; b and d are when the pump field is switched off.

Further, the evolution of $\alpha(\chi, \omega_p)$ with χ is more or less clearly seen in figure 2(a) in the whole range of variation of χ. At the same time, curves for large values of χ in figure 2(b) and in analogous figures of the OBE model are strongly pressed down to the frequency axis. So, the frequency dependence of $\alpha(\chi, \omega_p)$ in these cases at $\chi/2\pi = 200$ kHz is presented in figure 3 as an example.

From the curves presented in figures 2(a) and (b) and from analogous figures obtained in the OBE model, we have evaluated the HWHM $\delta\nu_{1/2}(\chi)$ of the holes for a set of values of χ. Data are displayed in figure 4 together with the theoretical FID results for the decay rate from figure 9 of [10] shown here for comparison purposes. Recall that here solid squares show the FID rate in the OBE model, solid circles are in the Redfield limit [2] and open circles represent our MBE FID data [10]. Experimental FID rate data of Boscaino and La Bella [2] (not shown) practically coincide with the latter [10]. Let us consider the field dependence of $\delta\nu_{1/2}$ in some detail.

It is seen that the OBE width in the presence of the pump field (open up triangles) at small χ is somewhat larger than the OBE FID rate (solid squares) and initially follows the latter with increasing χ. At $\chi/2\pi > 10$ kHz one observes a crossover from the Bloch to quasi-Redfield regime, but at much higher level than the ordinary Redfield one (solid circles in the figure). One can relate this last result to the contribution to the absorption due to the coherent interference between the pump and probe fields [15].

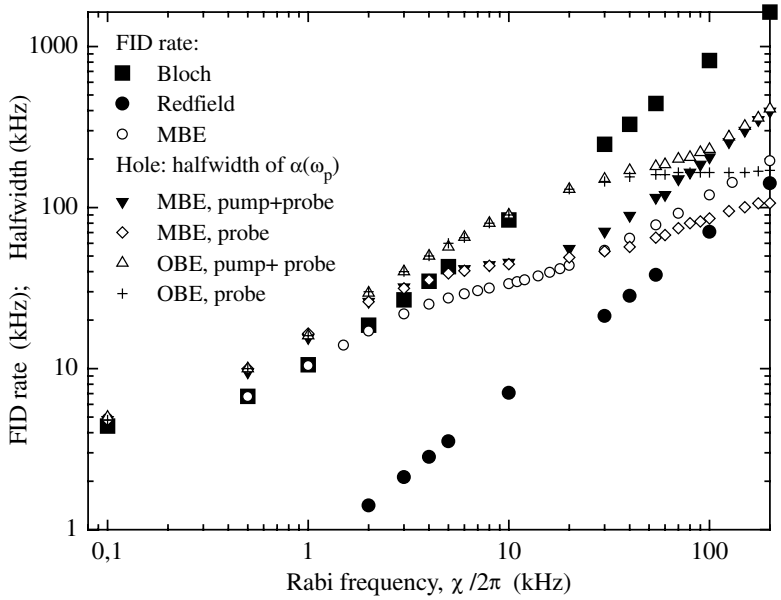

Figure 4. Half width at half minimum of the hole in the absorption spectrum of a probe field versus pump-field Rabi frequency, χ. 'MBE, pump + probe' is for a hole in the MBE model in the presence of the pump field and so on. Theoretical FID rate data [10] are given for comparison.

The OBE width in the absence of the pump field (crosses) follows the preceding result (OBE width in the presence of the pump field) till the crossover. At this stage, the former (crosses) is quickly saturated and is not changed further with increasing χ.

The field dependence of the MBE width in the presence of the pump field (solid down triangles) at small χ is similar to that of the OBE one. With increasing χ, a crossover from the Bloch to quasi-Redfield regime is observed at much lower level than that for the OBE width in the presence of the pump field (open up triangles) but at higher level than the crossover for FID rate in our MBE model (open circles). At very large χ, the MBE width in the presence of the pump field coincides with that for OBE one. Obviously, the difference between the MBE width and the MBE FID rate is caused, among other possible factors, mainly again by the coherent interference [15].

Finally, the MBE width in the absence of the pump field (open diamonds) repeats the MBE width in the presence of the pump field till the crossover; after the crossover the first rises much more slowly than the second and even more slowly than the MBE FID rate.

In the light of the above information about the hole width of the absorption coefficient, it is of some interest to consider the field dependence of the hole width for the polarization itself. Figure 5 presents the field dependence of the hole half width for the steady-state polarization in two different approximations: (i) for $(n_1 - n_2)(\omega)$, obtained in the kinetic-equation approximation by use of formulae (4) and (8) with the damping taken in the OBE model (T_2 and Δ are constants; solid diamonds) and in the our MBE model (T_2 and Δ are field-dependent; solid down triangles); (ii) for $w^{(0)}(\omega)$ (9), again in the OBE model (crosses) and in the MBE model (open up triangles). Of the four functional variables, only $w^{(0)}(\omega)$: MBE (open triangles) displays a crossover somewhat similar to that for the MBE FID rate (open circles).

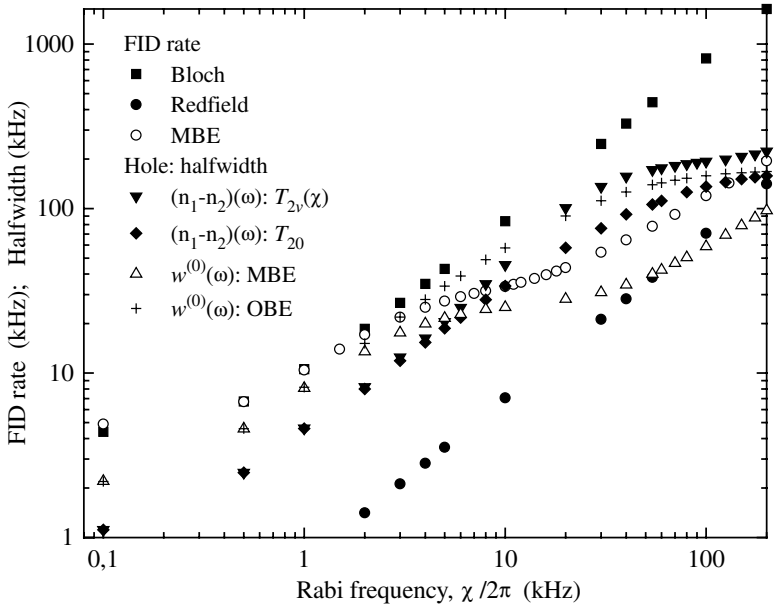

Figure 5. Half width at half minimum of the hole in the polarization spectrum versus pump-field Rabi frequency, χ. '$(n_1 - n_2)(\omega)$: $T_{2v}(\chi)$ (or T_{20})' is for a hole in the polarization spectrum in the kinetic-equation approximation (equation (8)) with the power-dependent relaxation parameter $T_{2v}(\chi)$ (or with the constant relaxation parameter $T_2 = T_{20}$). '$w^{(0)}(\omega)$' is for a hole in the polarization spectrum (equation (9)) in the MBE (OBE) model.

4. Conclusion

In a natural development of our work [10] on the modified Bloch equations, here they are applied to the hole-burning in the absorption spectrum of the two-level systems by steady-state excitation. We have derived general expressions for hole shapes in the presence of the pump field and when the latter is switched off. Detailed numerical calculations of the hole shapes and widths are carried out in the framework of the ordinary and the modified Bloch equations for a concrete system with known parameters involved in the calculations. Earlier this system was investigated successfully experimentally [1, 2] and theoretically [10] through transient nutations and free induction decay. It follows from figures 4 and 5 here and from [1, 2, 10] that the TN, FID and various hole-burning effects give somewhat different information about irreversible damping in the system.

Indeed, it was shown experimentally [1] that the TN decay is faster than expected from the OBE model. As is explained in [10], the TN decay is governed by large and intensity-dependent $\Gamma_{2v}(\chi, t)$; the Redfield–Tomita slowing down described by $\Gamma_{2u}(\chi)$ has a negligible effect.

In the steady-state prepared FID effect, the decay depends on both $\Gamma_{2u}(\chi)$ and $\Gamma_{2v}(\chi)$ [10]; however, it is to a great extent determined by the preparation process where parameter $\Gamma_{2u}(\chi)$ is of more importance than $\Gamma_{2v}(\chi)$. As a result, the FID decay rate $\Gamma(\chi)$ undergoes a crossover from the Bloch to Redfield regime (open circles in figures 4 and 5) [2, 10].

Finally, our results on the hole width in the MBE model are in qualitative agreement with the FID data. At the same time, there is important diversity in the intensity dependences of the FID decay rate and of the hole width, as one can see from figure 4. In this connection, there is obvious need in experiments on the hole burning in addition to those on the FID effect.

References

[1] Boscaino R, Gelardi F M and Korb J P 1993 *Phys. Rev.* B **48** 7077
[2] Boscaino R and La Bella M V 1990 *Phys. Rev.* A **41** 5171
[3] Boscaino R and Gelardi F M 1992 *Phys. Rev.* B **46** 14 550
[4] De Voe R G and Brewer R G 1983 *Phys. Rev. Lett.* **50** 1269
[5] Szabo A and Muramoto T 1989 *Phys. Rev.* A **39** 3992
[6] Yodh A G, Golub J, Carlson N W and Mossberg T W 1984 *Phys. Rev. Lett.* **53** 659
[7] Huang J, Zhang J M, Lezama A and Mossberg T W 1989 *Phys. Rev. Lett.* **63** 78
[8] Liu G K and Cone R L 1990 *Phys. Rev.* B **41** 6193
[9] Kroll S, Xu E Y, Kim M K, Mitsunaga M and Kachru R 1990 *Phys. Rev.* B **41** 11 568
[10] Asadullina N Ya, Asadullin T Ya and Asadullin Ya Ya 2001 *J. Phys.: Condens. Matter* **13** 3475
[11] Tomita K 1958 *Prog. Theor. Phys.* **19** 541
[12] Abragam A 1961 *The Principles of Nuclear Magnetism* (Oxford: Clarendon) ch 3
[13] Bloembergen N and Shen Y R 1964 *Phys. Rev.* **133** A37
[14] Agnello S, Boscaino R, Cannas M, Gelardi F M and Shakhmuratov R N 1999 *Phys. Rev.* A **59** 4087
[15] Letokhov V S and Chebotaev V P 1990 *Nonlinear Laser Spectroscopy of Super-High Resolution* (Moscow: Nauka) p 512 (in Russian)